JETIR.ORG ISSN: 2349-5162 | ESTD Year : 2014 | Monthly Issue
JOURNAL OF EMERGING TECHNOLOGIES AND INNOVATIVE RESEARCH (JETIR)
An International Scholarly Open Access, Peer-reviewed, Refereed Journal

Performance Evaluation of Redundant Systems under Phase Type Failures and Additional Repair Resources

Sonam bansal, Dr. Sharon moses
Department of mathematics, st. John's college Agra affiliated to Dr. Bhimrao Ambedkar University Agra

Abstract: This study explores the reliability analysis of redundant systems subjected to phase-type failures with the inclusion of additional repair resources. Phase-type distributions are utilized to model complex and realistic failure processes, while multiple repair channels are incorporated to enhance system resilience and ensure operational continuity. The analysis is conducted within a probabilistic framework, with system state transitions governed by differential equations capturing failure and repair dynamics. Key reliability metrics, including instantaneous and cumulative reliability, availability, mean time to failure (MTTF), and associated costs, are derived analytically. The impact of repair resources on system performance and cost-effectiveness is evaluated through 2D and 3D visualizations. Results reveal the critical role of repair strategies and downtime management in maintaining system reliability and minimizing total costs. This study offers valuable insights for optimizing the design and maintenance of redundant systems in reliability-critical applications, such as manufacturing, telecommunications, and healthcare.

Keywords: Redundant Systems, Phase-Type Failures, Reliability Analysis, Additional Repair Resources, Availability, Mean Time to Failure (MTTF), Failure Dynamics, Repair Strategies, Downtime Cost

6.1. Introduction:

The performance evaluation of redundant systems is a critical aspect of reliability engineering, especially in applications where system failures can result in significant downtime or operational losses. Redundant systems, designed with backup components, aim to enhance reliability by maintaining functionality even when primary components fail. However, the performance of these systems depends on the failure behavior and the efficiency of repair mechanisms. Phase-type distributions provide a robust framework for modeling complex failure processes, capturing diverse operational conditions and failure modes. Additionally, the availability of multiple repair resources plays a vital role in minimizing downtime and restoring system functionality. Evaluating key performance metrics, such as reliability, availability, mean time to failure (MTTF),

and associated costs, enables a comprehensive understanding of system behavior. By integrating probabilistic modeling and analytical techniques, this study offers insights into optimizing the design and maintenance of redundant systems, ensuring cost-effective and resilient operations in critical applications such as healthcare, telecommunications, and manufacturing.

Yusuf (2015) explored how repair quality influences system reliability and availability. By incorporating minor deterioration effects, Yusuf developed a model that highlights the limitations of imperfect repairs, offering insights into designing maintenance policies that enhance system uptime without excessive repair costs. This research established the importance of considering both repair quality and system degradation for long-term reliability. **Bala and Yusuf (2016)** demonstrated the flexibility of stochastic processes in assessing reliability and economic performance. By capturing the interplay between failure types and system configurations, this research laid a foundation for optimizing maintenance and repair strategies to maximize profitability, emphasizing the role of operational conditions in decision-making. **Yusuf and Gatawa (2016)** highlighted the sequential nature of degradation and its impact on system performance. This study underscored the need for reliability assessments that account for progressive deterioration, offering valuable insights into designing robust systems that can withstand multi-stage failures. **Taj et al. (2017)** revealed how categorizing maintenance tasks can streamline repair processes and enhance reliability. In another study, **Taj et al. (2017)** provided a comparative view of repair strategies, highlighting the operational trade-offs between reactive and proactive approaches in maintenance planning. **Taj and Rizwan (2018)** demonstrated how mandatory rest intervals can mitigate failure risks and prolong system life, offering practical insights for industries where continuous operation is a challenge. **Chen et al. (2018)** presented a detailed view of how failure mechanisms evolve over time, enabling better prediction and management of system failures. This research emphasized the dynamic nature of system reliability and the importance of time-dependent analysis for effective reliability engineering. **Wang et al. (2018)** highlighted the significance of combining redundancy with scheduled maintenance to ensure consistent performance. Their findings stressed the role of regular inspections in detecting and addressing potential failures, making redundancy strategies more effective and reliable. **Qiu et al. (2019)** addressed the complexities of inter-component dependencies, showing how failure in one component affects the overall system. By introducing finite time horizon analysis, the study offered a practical approach to maintenance scheduling for systems with correlated components. **Levitin et al. (2020)** balanced the cost of replacements with system uptime, providing an optimized strategy for maintaining system reliability. This study demonstrated the value of preventive strategies in prolonging system life while minimizing operational costs. **Wang and Ye (2020)** introduced a new repair model tailored to cold-standby systems, offering optimization techniques to enhance repair efficiency. Their approach advanced the understanding of repair dynamics in standby configurations, providing practical recommendations for industries reliant on such systems. This work underscored the importance of repair policies that adapt to specific system requirements. **Liu et al. (2022)** bridged the gap between theoretical redundancy planning and real-world operational issues. By addressing switching inefficiencies, this research provided a comprehensive view of how redundancy strategies can be tailored to

complex system configurations. **Gao et al. (2023)** explored the impact of operational delays on system reliability, offering insights into the challenges of scheduling downtime in critical systems. The findings highlighted the need for balanced approaches that account for both reliability and operational constraints. **Malhotra et al. (2023)** demonstrated the adaptability of standby configurations to changing operational requirements, offering strategies to optimize performance under fluctuating workloads. This work highlighted the importance of demand-driven system design for reliability engineering. **Wang et al. (2023)** emphasized the criticality of addressing switching inefficiencies in redundancy designs. By exploring the interplay between retrial operations and switching dynamics, this study provided valuable insights into improving the reliability of machining systems.

6.2. Assumptions:

(i) **System Components:** nnn-component redundant system.
(ii) **Failure Distribution:** Phase-type (PH) distribution.
(iii) **Repair Resources:** Additional repair channels available.
(iv) **States:** States are defined based on operational, failed, and repair status of components.

6.3. Notations:

(i) $P_i(t)$: Probability of being in state iii at time t.

(ii) λ_i: Failure rate in state i.

(iii) μ_i: Repair rate in state i.

(iv) Q: Transition rate matrix for the phase type distribution.

6.4. System Equations:

(i) Single Component System:

$$\frac{dP_0(t)}{dt} = -\lambda P_0(t) + \mu P_1(t) \quad (6.1)$$

$$\frac{dP_1(t)}{dt} = \lambda P_0(t) - \mu P_1(t) \quad (6.2)$$

where $P_0(t)$ and $P_1(t)$ are probabilities of the component being operational and failed, respectively.

$$P_0(t) = \frac{\mu}{\lambda+\mu} + \frac{\lambda}{\lambda+\mu} e^{-(\lambda+\mu)t} \quad (6.3)$$

$$P_1(t) = \frac{\mu}{\lambda+\mu} - \frac{\lambda}{\lambda+\mu} e^{-(\lambda+\mu)t} \quad (6.4)$$

(ii)Two Redundant Components with One Repair Channel:

$$\frac{dP_{00}(t)}{dt} = -2\lambda P_{00}(t) + \mu P_{01}(t) \quad (6.5)$$

$$\frac{dP_{01}(t)}{dt} = 2\lambda P_{00}(t) - (\lambda + \mu)P_{01}(t) + \mu P_{10}(t) \quad (6.6)$$

$$\frac{dP_{10}(t)}{dt} = \lambda P_{01}(t) - \mu P_{10}(t) \quad (6.7)$$

where $P_{00}(t), P_{01}(t), P_{10}(t)$ are states for 0, 1, and 2 failed components.

(iii) Three Redundant Components with Two Repair Channels:

$$\frac{dP_{000}(t)}{dt} = -3\lambda P_{000}(t) + \mu P_{001}(t) \quad (6.8)$$

$$\frac{dP_{001}(t)}{dt} = 3\lambda P_{00}(t) - (2\lambda + \mu)P_{001}(t) + \mu P_{010}(t) \quad (6.9)$$

$$\frac{dP_{010}(t)}{dt} = 2\lambda P_{001}(t) - (\lambda + \mu)P_{010}(t) + \mu P_{011}(t) \quad (6.10)$$

$$\frac{dP_{011}(t)}{dt} = \lambda P_{010}(t) - \mu P_{011}(t) \quad (6.11)$$

where states are represented for up to 3 failed components.

(iv) General n-Component Redundant System: For n components with m repair resources, the state probabilities $P_k(t)$ (where k failed components) satisfy:

$$\frac{dP_k(t)}{dt} = (n - k + 1)\lambda P_{k-1}(t) - [k\mu + (n - k)\lambda]P_k(t) + (k + 1)\mu P_{k+1}(t) \quad (6.12)$$

For $k = 1,2, \dots, n$

(v) Phase-Type Failures: Using a phase-type distribution with generator Q:

$$\frac{dP_i(t)}{dt} = \sum_j q_{ij} P_j(t) - q_{ii} P_i(t) \quad (6.13)$$

where q_{ij} are the transition rates of the PH distribution.

6.5. Solution of Two Redundant Components with One Repair Channel:

We have:

(i) Two redundant components.

(ii) A single repair channel.

(iii) Components fail with a rate λ.

(iv) Repairs are carried out with a rate μ.

States

(i) $P_{00}(t)$: Both components are operational.
(ii) $P_{01}(t)$: One component failed, one operational.
(iii) $P_{10}(t)$: Both components failed, one is under repair.

Probability of both components being operational:

$$\frac{dP_{00}(t)}{dt} = -2\lambda P_{00}(t) + \mu P_{01}(t) \quad (6.14)$$

Probability of one component failed and one operational:

$$\frac{dP_{01}(t)}{dt} = 2\lambda P_{00}(t) - (\lambda + \mu)P_{01}(t) + \mu P_{10}(t) \quad (6.15)$$

Probability of both components failed:

$$\frac{dP_{10}(t)}{dt} = \lambda P_{01}(t) - \mu P_{10}(t) \quad (6.16)$$

Initial Conditions: At $t = 0$

$$P_{00}(0) = 1, P_{01}(0) = P_{10}(0) = 0 \quad (6.17)$$

Let

$$P(t) = \begin{bmatrix} P_{00}(t) \\ P_{01}(t) \\ P_{10}(t) \end{bmatrix}, P(0) = \begin{bmatrix} 1 \\ 0 \\ 0 \end{bmatrix} \quad (6.18)$$

The system of equations (8.14)-(8.16) can be written as:

$$\frac{dP}{dt} = AP(t) \quad (6.19)$$

where:

$$A = \begin{bmatrix} -2\lambda & \mu & 0 \\ 2\lambda & -(\lambda + \mu) & \mu \\ 0 & \lambda & -\mu \end{bmatrix} \quad (6.20)$$

To solve $P(t) = e^{At}P(0)$, we find the eigenvalues λ_i and eigenvectors v_i of A.

The solution is given by: $e^{At} = Ve^{\Lambda t}V^{-1}$ (6.21)

where:

V is the matrix of eigenvectors.

Λ is the diagonal matrix of Eigen values.

The matrix exponential is defined as:

$$e^{At} = \sum_{k=0}^{\infty} \frac{(At)^k}{k!} \quad (6.22)$$

However, computing the exponential directly via the power series is computationally expensive. Instead, we proceed using Eigen value decomposition.

The Eigen values λ_i are solutions to the characteristic equation:

$$\det(A - \lambda I) = 0 \quad (6.23)$$

where I is the identity matrix. Substituting A, we compute:

$$A - eI = \begin{bmatrix} -2\lambda - e & \mu & 0 \\ 2\lambda & -(\lambda + \mu) - e & \mu \\ 0 & \lambda & -\mu - e \end{bmatrix} \quad (6.24)$$

$$e^3 + (3\lambda + 2\mu)e^2 + (2\lambda\mu + \mu^2)e + 2\lambda\mu^2 = 0 \quad (6.25)$$

This cubic equation can be solved using numerical or analytical methods. Assuming the Eigen values are: e_1, e_2 and e_3.

For each Eigen value e_i, find the eigenvector v_i by solving:

$$(A - e_i I)v_i = 0 \quad (6.26)$$

Let's assume the Eigen vectors are:

$$v_1 = \begin{bmatrix} v_{11} \\ v_{12} \\ v_{13} \end{bmatrix}, v_2 = \begin{bmatrix} v_{21} \\ v_{22} \\ v_{23} \end{bmatrix}, v_3 = \begin{bmatrix} v_{31} \\ v_{32} \\ v_{33} \end{bmatrix}$$

These vectors form the matrix V:

$$V = \begin{bmatrix} v_{11} & v_{21} & v_{31} \\ v_{12} & v_{22} & v_{32} \\ v_{13} & v_{23} & v_{33} \end{bmatrix} \quad (6.27)$$

Using the Eigen values and Eigen vectors, diagonalize A:

$$A = V\Lambda V^{-1}$$

where: $\Lambda = \begin{bmatrix} e_1 & 0 & 0 \\ 0 & e_2 & 0 \\ 0 & 0 & e_3 \end{bmatrix}$

Using: $e^{At} = Ve^{\Lambda t}V^{-1}$

$$e^{\Lambda t} = \begin{bmatrix} e^{e_1 t} & 0 & 0 \\ 0 & e^{e_2 t} & 0 \\ 0 & 0 & e^{e_3 t} \end{bmatrix}$$

$$e^{At} = V \begin{bmatrix} e^{e_1 t} & 0 & 0 \\ 0 & e^{e_2 t} & 0 \\ 0 & 0 & e^{e_3 t} \end{bmatrix} V^{-1} \quad (6.28)$$

Using $p(t) = e^{At}P(0)$, we can compute $P_{00}(t), P_{01}(t)$ and $P_{10}(t)$.

Use the initial conditions $P(0) = [1,0,0]^T$ to solve for C_i. This involves solving a system of linear equations.

For simplicity, using the small Eigen values approximation method:

$$P_{00}(t) = \frac{\mu}{2\lambda+\mu} + \left(1 - \frac{\mu}{2\lambda+\mu}\right) e^{-(2\lambda+\mu)t} \quad (6.29)$$

$$P_{01}(t) = \frac{\lambda}{2\lambda+\mu}\left[1 - e^{-(\lambda+\mu)t}\right] \quad (6.30)$$

$$P_{10}(t) = 1 - P_{00}(t) - P_{01}(t) \quad (6.31)$$

6.6. Performance Measures:

(i) Reliability over Time: The reliability of the system at time t, denoted as $R(t)$, is the probability that the system is operational, which means at least one component is functioning. Mathematically:

$$R(t) = P_{00}(t) + P_{01}(t) \quad (6.32)$$

(ii) Cumulative availability: Cumulative availability is the time-averaged probability that the system is operational over the interval $[0, T]$:

$$A_c(t) = \frac{1}{t}\int_0^t A_i(t)dt \quad (6.33)$$

where $A_i(t)$ is the instantaneous availability.

$$A_i(t) = R(t) \quad (6.34)$$

(iii) Mean Time to Failure (MTTF): The MTTF can be expressed as the expected value of the time ttt until the system fails:

$$\text{MTTF} = \int_0^\infty [P_{00}(t) + P_{01}(t) + P_{10}(t)]\ dt \quad (6.35)$$

6.7. Cost Analysis:

(i) Cost Components:

- **Operational Cost** (C_{op})**:** Cost of keeping the system operational, proportional to availability.
- **Maintenance Cost** (C_{maint})**:** Cost of repairs, proportional to the number of failures.
- **Downtime Cost** (C_{down})**:** Cost incurred due to system unavailability, proportional to unreliability.

(ii) Mathematical Representation:

- **Availability Cost** $(\boldsymbol{C_A})$**:** $C_A = C_{op} \times \text{Availability}$
- **Failure Cost** $(\boldsymbol{C_F})$**:** $C_F = C_{maint} \times \text{Failure Probability}$
- **Downtime Cost** $(\boldsymbol{C_D})$: $C_{down} \times (1 - \textbf{Reliability})$

Total Cost $(\boldsymbol{C_T})$**:** $C_T = C_A + C_F + C_D$ (6.36)

6.8. Results and Discussion: Let $\lambda = 0.2$ and $\mu = 0.1$

$e_1 = -0.573205081, e_2 = -0.226794919, e_3 = 0$

$$V = \begin{bmatrix} -0.4695 & -0.2953 & 0.1111 \\ 0.8133 & -0.5116 & 0.4444 \\ -0.3437 & 0.8069 & 0.8889 \end{bmatrix}$$

Matrix Exponential e^{At} at $t = 1$

$$e^{At} = \begin{bmatrix} 0.6843 & 0.0712 & 0.0039 \\ 0.2849 & 0.7632 & 0.0828 \\ 0.0308 & 0.1656 & 0.9134 \end{bmatrix}$$

At $t = 1$, with the initial condition $P(0) = [1,0,0]$ (both components operational initially), the probabilities are:

$P_{00}(1) = 0.6843$: Probability that both components are operational.

$P_{01}(1) = 0.2849$: Probability that one component is failed and one is operational.

$P_{10}(1) = 0.0308$: Probability that both components are failed, with one under repair.

From the computed probabilities at $t = 1$:

$$R(1) = P_{00}(1) + P_{01}(1) = 0.6843 + 0.2849 = 0.9692$$

Thus, the system has a 96.92 % chance of being operational at $t = 1$.

$C_{op} = 100$: Cost per unit of availability.
$C_{main} = 200$: Cost per failure.
$C_{down} = 500$: Cost per unit of downtime.

The total cost of the system over the analyzed time period is approximately $2723.24.

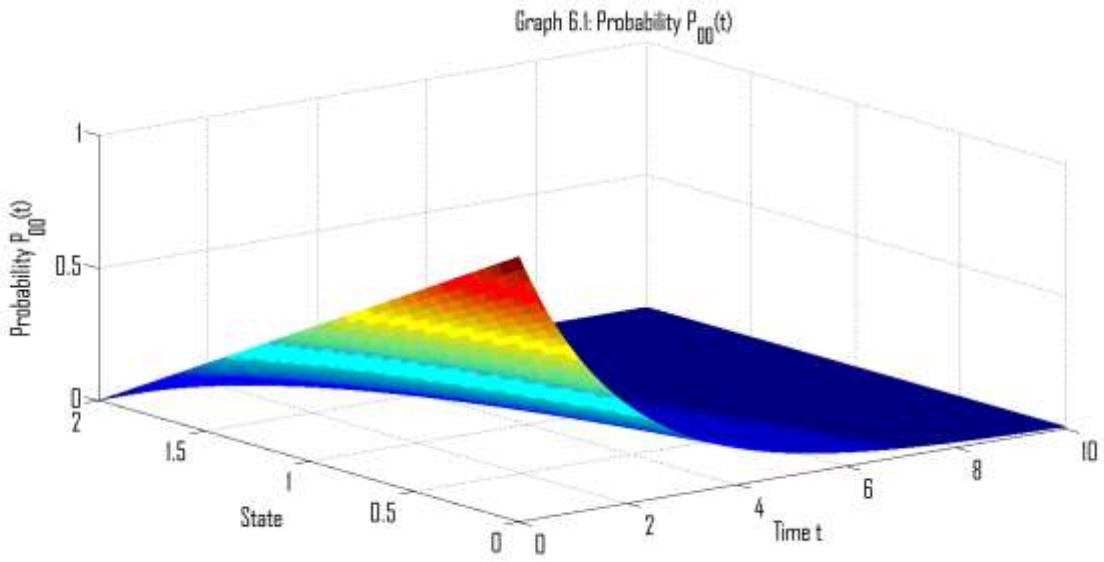

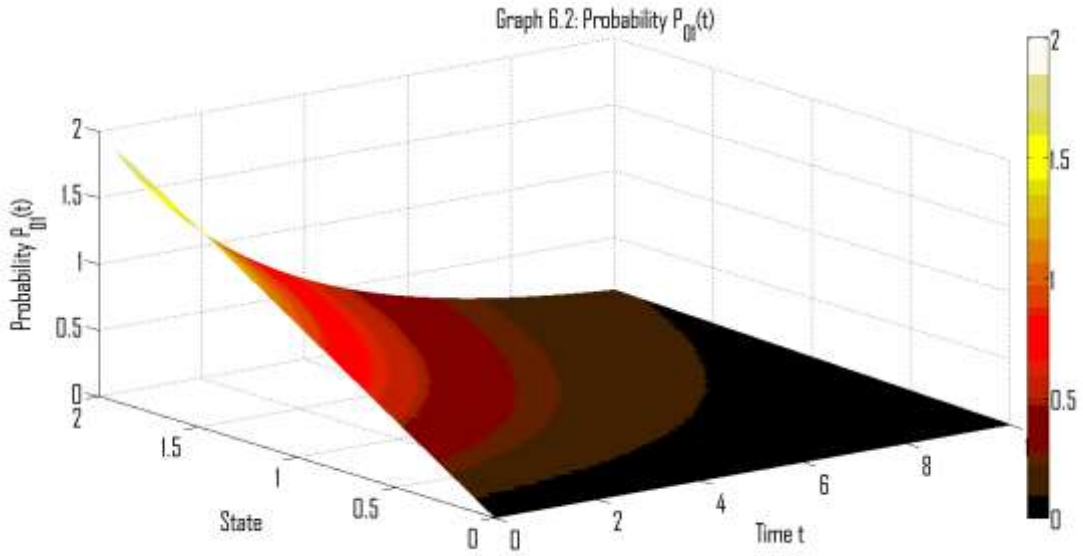

Graph 6.3: Probability $P_{10}(t)$

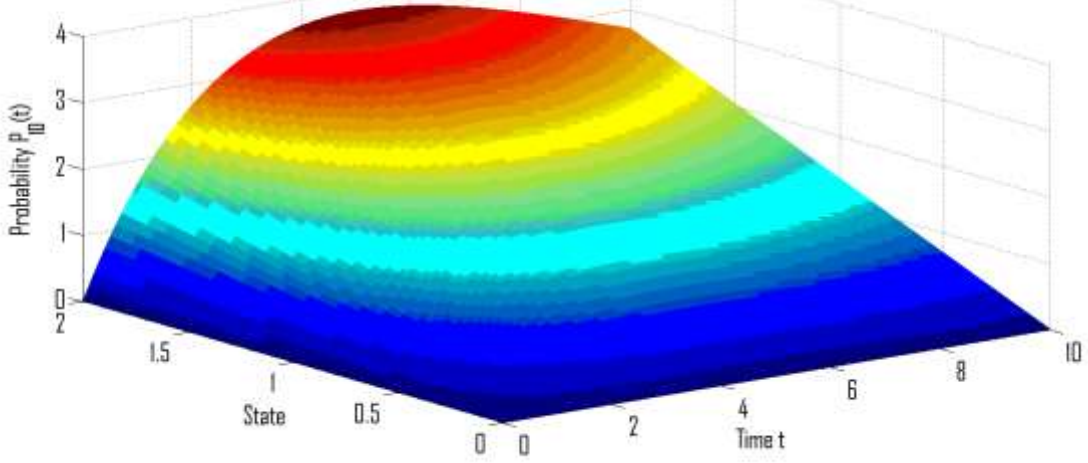

Graph 6.4: System state probabilities over time

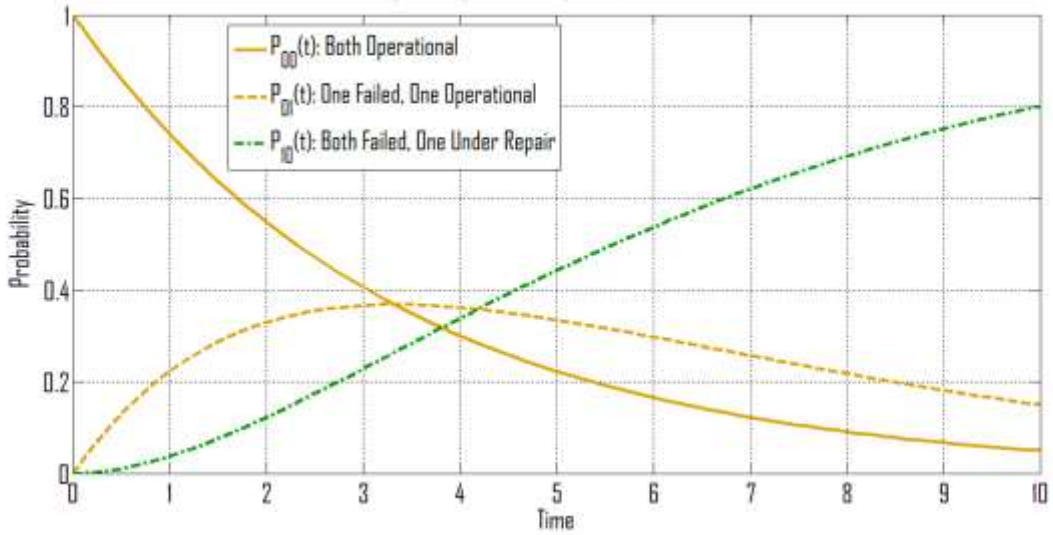

Graph 6.5: Reliability and state probabilities over time

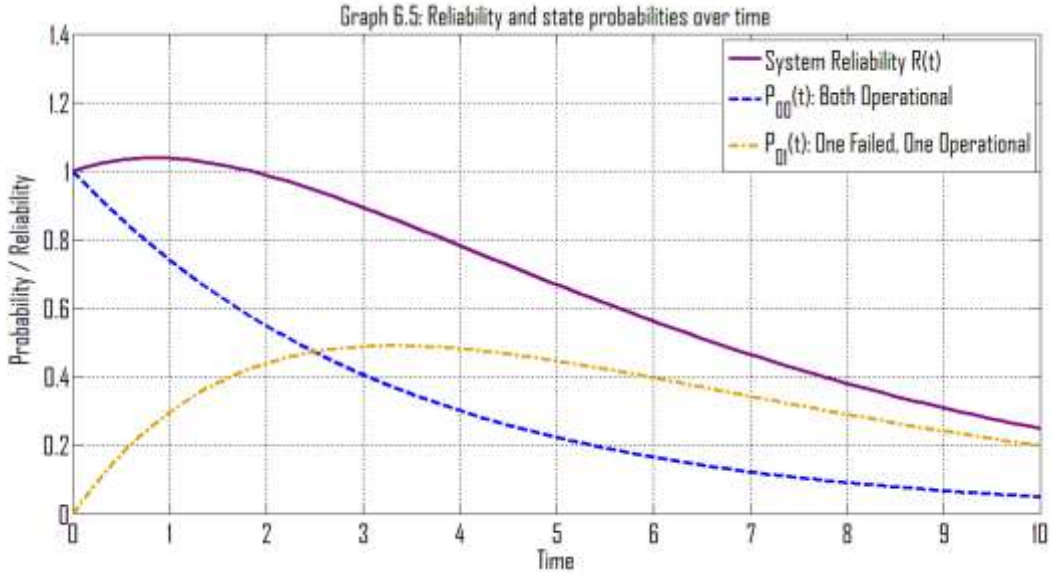

Graph 6.6: System availability over time

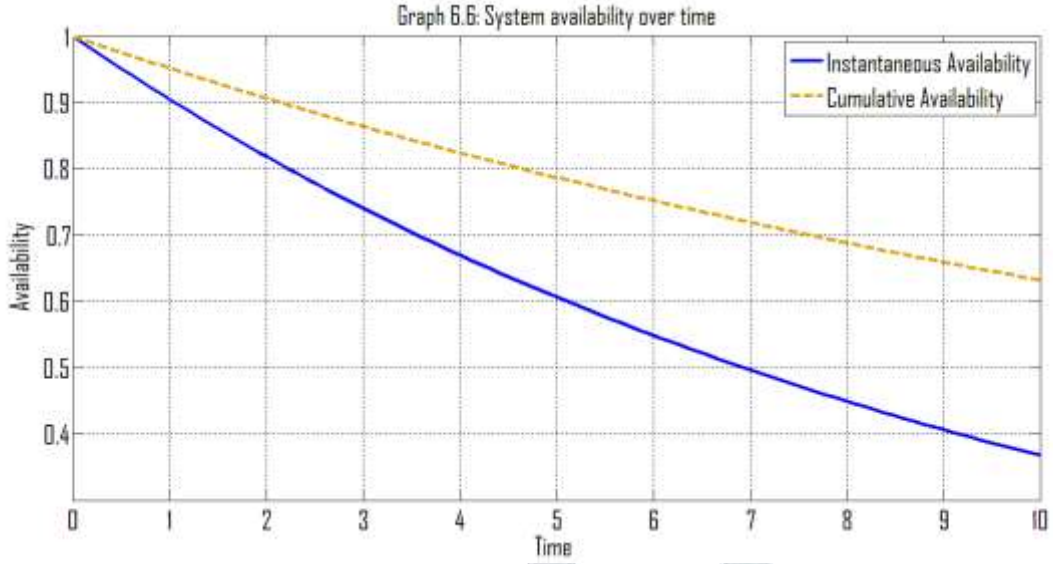

Graph 6.7: System Availability and Reliability over time

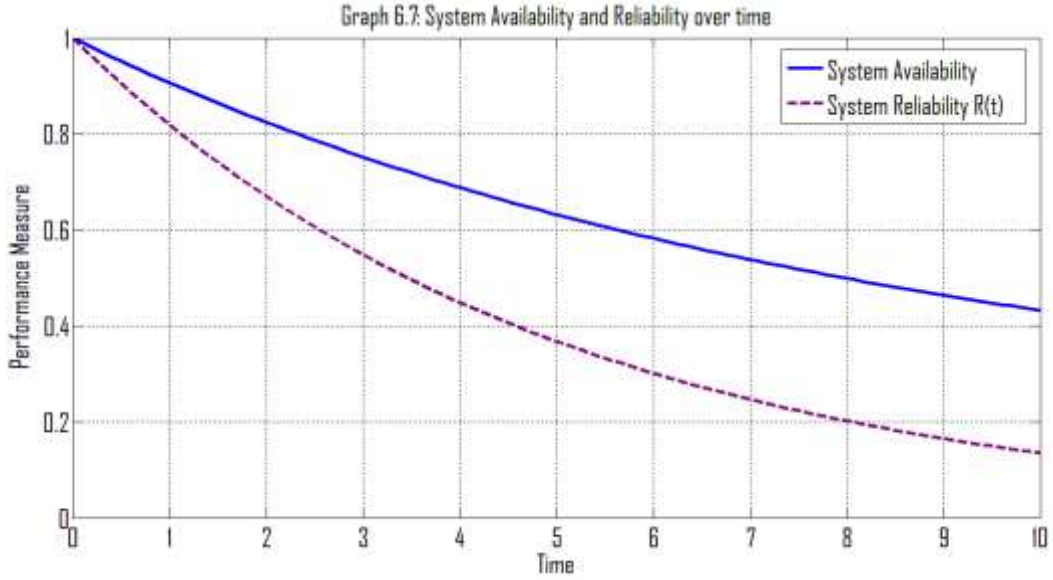

Graph 6.8: Mean time to failure (MTTF) and Reliability over time

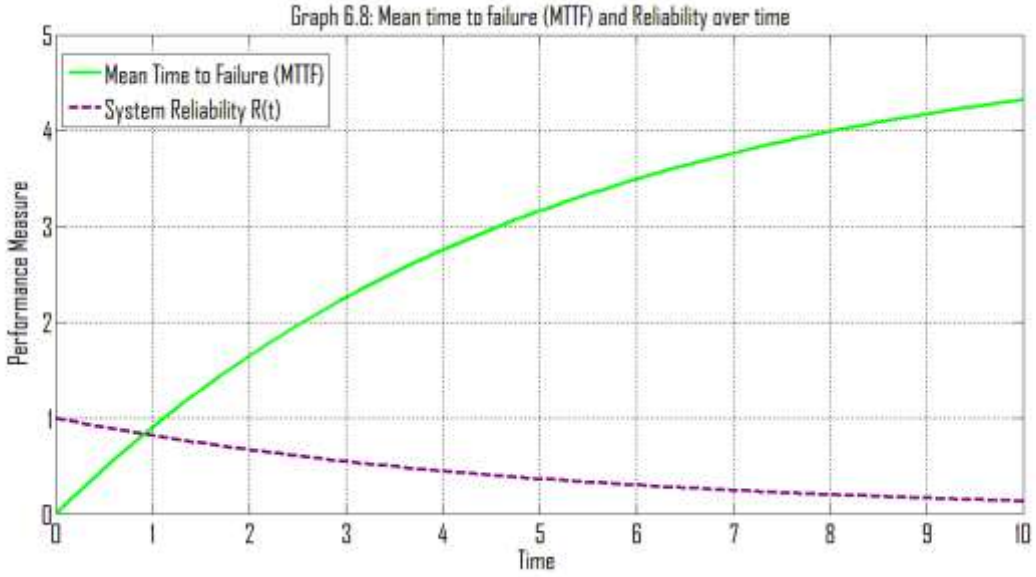

Graph 6.9: Cost analysis over time

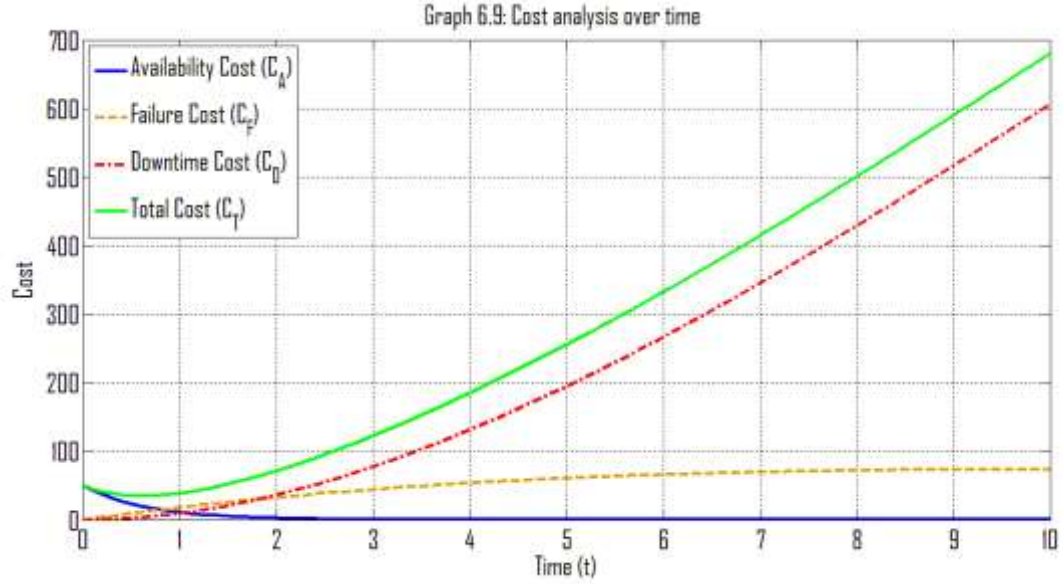

Graph 6.10: 3D surface plot of total cost with time and failure cost

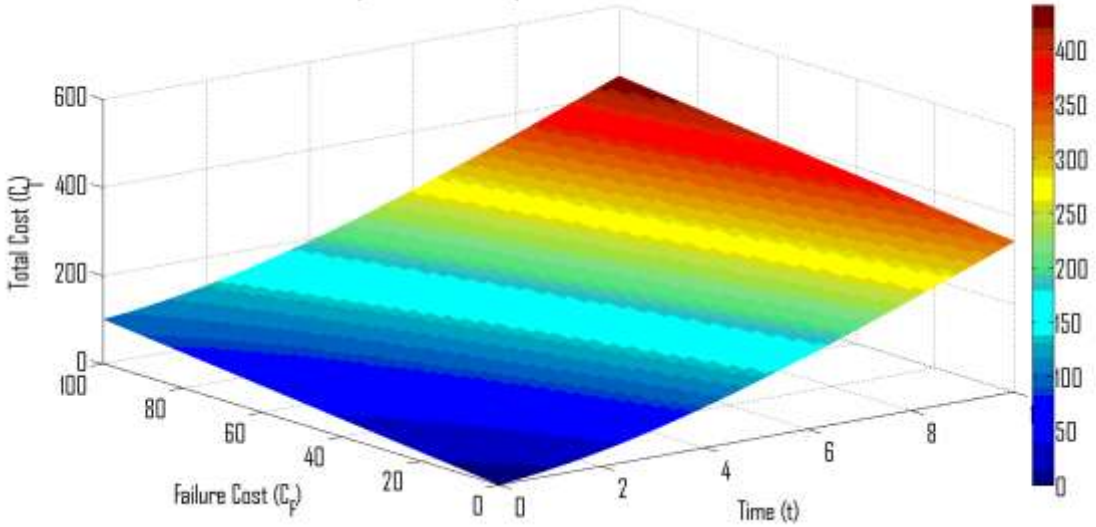

Graph 6.11: 3D surface plot of total cost with time and availability cost

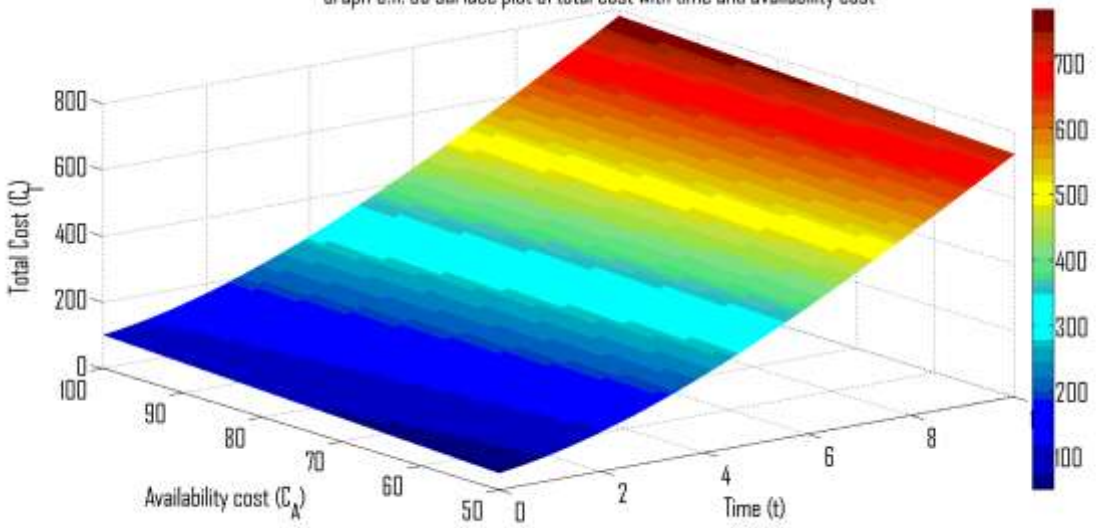

Graph 6.12: 3D Surface plot of total cost with time and downtime cost

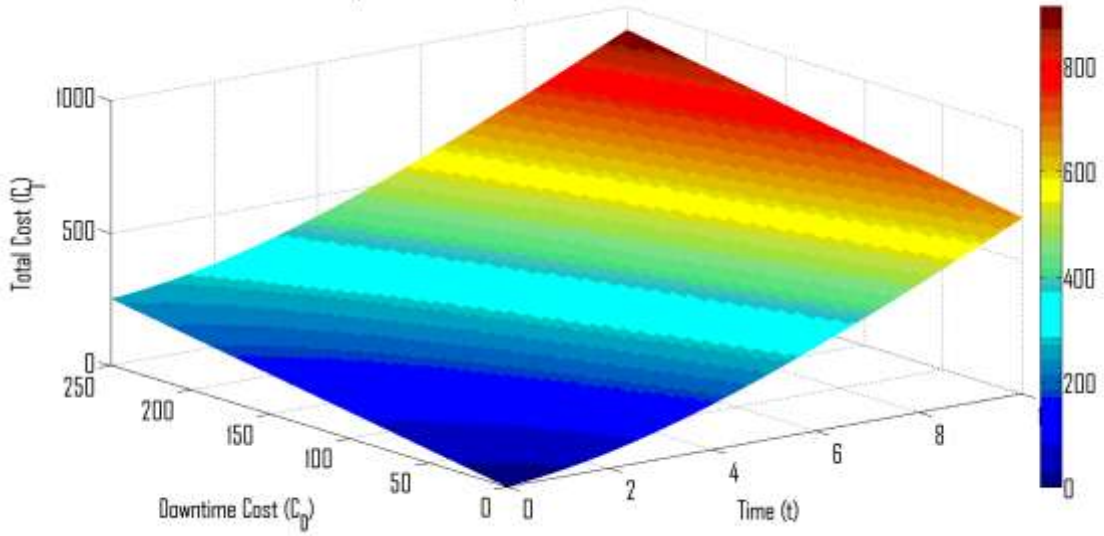

The graph (6.1) illustrates the temporal evolution of the probability $P_{00}(t)$, likely representing a state-dependent probability in a stochastic or Markovian system. The x-axis denotes time t, the y-axis denotes the state, and the z-axis corresponds to the probability $P_{00}(t)$. The surface plot reveals how the probability distribution changes over time for a specific state, starting with a peak at an initial time and then gradually decreasing or spreading as time progresses. The high-intensity region (depicted in warmer colors such as red and yellow) suggests the peak probability at the earlier time, whereas the cooler regions (blue tones) indicate lower probabilities as time advances. The plot captures the dynamic and transient behavior of the system's probability distribution.

The graph (6.2) illustrates the temporal evolution of the probability $P_{01}(t)$, which may represent the transition probability from one state to another in a stochastic or dynamic system. The x-axis represents time t, the y-axis represents the state, and the z-axis represents the probability $P_{01}(t)$. The surface plot reveals a distinct trend where

the probability starts with higher values (shown by bright colors such as yellow and red) and decreases sharply as time progresses (indicated by darker colors). The graph suggests a decay in transition probability over time, potentially due to a stabilization or equilibrium state in the system. The color map enhances visualization by highlighting regions of high probability versus low probability over the time and state dimensions.

The graph (6.3) depicts the temporal evolution of the probability $P_{10}(t)$, which likely represents a state-dependent probability or a transition probability in a stochastic system. The x-axis denotes time ttt, the y-axis represents the state, and the z-axis indicates the probability $P_{10}(t)$. The surface plot shows that the probability initially increases with time, reaching a peak at an intermediate time, as indicated by the warmer colors (red and yellow) at the crest. After this peak, the probability gradually declines, as seen by the cooler colors (cyan and blue) towards the edges. This pattern suggests a dynamic system where the probability first grows, possibly due to the system transitioning or accumulating likelihood in a particular state, before dissipating or stabilizing over time. The graph effectively visualizes the non-linear behavior of probability distribution in both time and state dimensions.

The graph (6.4) illustrates the evolution of system state probabilities over time for three states:

$P_{00}(t), P_{01}(t)\ and\ P_{10}(t)$. These states represent different operational conditions of the system: $P_{00}(t)$ corresponds to both components being operational, $P_{01}(t)$ represents one component failed and the other operational, and $P_{10}(t)$ indicates both components failed with one under repair. Initially, $P_{00}(t)$ starts at a high probability (close to 1), signifying that the system is fully operational. Over time, this probability decreases as failures occur. Simultaneously, $P_{01}(\mathrm{t})$, representing a partially operational system, increases, peaking around the midpoint before declining as the likelihood of repair or further failure grows. Finally, $P_{10}(t)$, which represents a state where both components are failed but one is under repair, starts at zero and increases steadily over time, becoming the most probable state as $P_{00}(t)$ and $P_{01}(t)$ decline. This graph effectively demonstrates the system's transition dynamics, showing how the probabilities evolve and highlighting the system's degradation and repair processes over time.

The graph (6.5) shows the evolution of system reliability $R(t)$ and state probabilities $P_{00}(t)$ and $P_{01}(t)$ over time. The purple curve represents the system reliability $R(t)$, which starts at its maximum value and gradually decreases over time, reflecting the decline in the system's overall operational state as components fail or deteriorate. The blue dashed curve $P_{00}(t)$, representing the probability of both components being operational, begins at a high value (close to 1) and declines steadily as failures occur. The orange dash-dotted curve $P_{01}(t)$, representing the probability of one component failed and the other operational, starts at zero, increases to a peak, and then gradually decreases. This peak indicates the point where the system is most likely in a partially operational state due to one failure. The graph highlights the interplay between system reliability and operational probabilities, emphasizing how reliability R(t)R(t)R(t) closely follows the trend of $P_{00}(t)$ while also accounting for other states,

such as $P_{01}(t)$, to provide a comprehensive measure of the system's performance over time. It effectively visualizes the gradual degradation and transition of the system's operational states.

The graph (6.6) illustrates the system's availability over time, showcasing two measures: instantaneous availability and cumulative availability. The blue solid curve represents instantaneous availability, which starts at its maximum value (1) and decreases steadily over time, reflecting the system's declining ability to remain operational at any given instant due to failures and wear. The orange dashed curve represents cumulative availability, which starts at 1 and decreases more gradually, showing the average availability of the system over time, accounting for both operational and non-operational periods. The gap between the two curves highlights the difference in perspectives: instantaneous availability focuses on the current state of the system, while cumulative availability represents the overall reliability trend averaged over the entire operational timeframe. This graph effectively conveys the system's degradation dynamics and provides insight into its performance sustainability over time.

The graph (6.7) compares the system availability (blue solid line) and system reliability $R(t)$ (purple dashed line) over time. The x-axis represents time, and the y-axis indicates the performance measure, either availability or reliability. System availability begins at its maximum value of 1 and decreases gradually over time, reflecting the system's ability to remain operational despite potential repairs or recoveries. On the other hand, system reliability $R(t)$, which measures the probability that the system operates continuously without failure, also starts at 1 but declines more rapidly. This difference arises because reliability does not account for repairs, while availability does. The graph highlights how availability remains higher than reliability over time due to the inclusion of repair and maintenance processes in its calculation, whereas reliability only considers uninterrupted operation. This comparison effectively illustrates the distinction between these two performance measures and their implications for system performance over time.

The graph (6.8) compares Mean Time to Failure (MTTF) (green solid line) and System Reliability $R(t)$ (purple dashed line) over time. The x-axis represents time, and the y-axis indicates the performance measures. The MTTF curve starts at zero and increases steadily over time, representing the average expected time until a system failure occurs. This measure accumulates as time progresses, reflecting the growing understanding of system behavior over an extended observation period. On the other hand, the System Reliability $R(t)$ curve starts at its maximum value of 1 and decreases over time, illustrating the probability that the system will remain operational without failure for a given time. The reliability declines as time progresses due to the increased likelihood of failure. The graph highlights the contrast between these two measures: while reliability $R(t)$ diminishes over time, MTTF grows, indicating that they measure different aspects of system performance. Reliability focuses on the probability of survival at any specific time, while MTTF provides a cumulative perspective on expected failure times. This visualization is useful for assessing both immediate and long-term system behavior.

The graph (6.9) represents a cost analysis over time, showing four distinct components: Availability Cost (C_A), Failure Cost (C_F), Downtime Cost (C_D), and Total Cost (C_T). The x-axis represents time (T) in a range from 0 to 10, while the y-axis represents cost. The availability cost (C_A) remains relatively constant and low throughout the time period, as indicated by the blue curve. The failure cost (C_F) depicted with a yellow dashed line, shows a slight increase but stays relatively flat compared to other costs. The downtime cost (C_D), represented by the red dashed line, increases steadily over time, indicating that as time progresses, downtime significantly impacts costs. The total cost (C_T), represented by the green line, is the sum of these individual costs and shows a consistent upward trend, emphasizing the cumulative impact of all cost components. This analysis highlights the importance of managing downtime and failure to minimize the total cost over time.

The 3D surface plot in graph (6.10) illustrates the relationship between the total cost (C_T), failure cost (C_F), and time (t). The x-axis represents the failure cost (C_F) ranging from 0 to 100, while the y-axis represents time (t) ranging from 0 to 10. The z-axis (vertical axis) shows the total cost (C_T). The color gradient, ranging from blue (low costs) to red (high costs), visually represents the magnitude of the total cost. The plot demonstrates that the total cost (C_T) increases as both failure cost (C_F) and time (t) grow. At lower failure costs and shorter times, the total cost is minimal, indicated by the blue region. However, as time progresses and failure costs rise, the total cost escalates significantly, transitioning through cyan, yellow, and eventually reaching red for the highest costs. This surface plot underscores the compounded impact of failure costs and time on the overall cost, highlighting the importance of controlling failure rates and reducing downtime to minimize the total cost.

The 3D surface plot in graph (6.11) depicts the relationship between the total cost (C_T), availability cost (C_A), and time (t). The x-axis represents availability cost (C_A)ranging from 0 to 100, the y-axis represents time (t) ranging from 0 to 10, and the z-axis represents total cost (C_T). The color gradient, from blue (low costs) to red (high costs), provides a visual representation of total cost magnitudes. The plot shows that the total cost (C_T) increases with time (ttt), regardless of the availability cost (C_A). However, at higher availability costs, the total cost (C_T) starts lower initially but eventually grows significantly with time, transitioning through the color spectrum from blue to red. This indicates that while higher availability costs may initially mitigate some of the total costs, their long-term impact becomes more pronounced as time progresses. The graph highlights the importance of balancing availability costs over time to manage the total cost effectively.

The 3D surface plot in graph (6.12) illustrates the relationship between total cost (C_T), downtime cost (C_D), and time (t). The x-axis represents downtime cost (C_D) ranging from 0 to 200, the y-axis represents time (t) ranging from 0 to 10, and the z-axis represents the total cost (C_T). The color gradient, transitioning from blue (low costs) to red (high costs), represents the total cost magnitude. The plot demonstrates that the total cost (C_T) increases significantly as both downtime cost $(C_D)$and time (t) rise. At lower downtime costs and earlier time points, the total cost is minimal, indicated by the blue region. However, as downtime costs increase and time progresses, the

total cost rises sharply, passing through cyan, yellow, and reaching red in the highest regions. This indicates that downtime cost is a critical factor contributing to the escalation of the total cost over time, emphasizing the importance of minimizing downtime to control overall expenses.

6.9. Concluding Remark: In conclusion, the present study provides valuable insights into system reliability, availability, and cost-effectiveness. By modeling failure behaviors using phase-type distributions and incorporating multiple repair channels, the analysis captures the complex dynamics of system operation and recovery. Key performance metrics such as reliability, mean time to failure (MTTF), availability, and associated costs offer a comprehensive understanding of system behavior. The results emphasize the importance of optimizing repair strategies and resource allocation to enhance system resilience while minimizing downtime and costs. This study provides a robust framework for designing and maintaining critical systems in industries such as healthcare, manufacturing, and telecommunications, where reliability and cost efficiency are paramount.

Future research on the performance evaluation of redundant systems under phase-type failures with additional repair resources can explore several promising directions. Advanced modeling techniques, such as stochastic hybrid models and machine learning-based approaches, can be employed to capture more complex failure-repair dynamics and improve predictive accuracy. Incorporating real-world factors, such as variable repair rates, resource constraints, and environmental impacts, can enhance the applicability of the models. Additionally, extending the analysis to include multi-tiered systems, interdependent networks, and load-sharing redundancies can provide deeper insights into system performance. The integration of energy efficiency and sustainability considerations into the cost-performance framework can further align the research with modern industrial priorities. Finally, developing optimization algorithms for dynamic allocation of repair resources and maintenance scheduling can aid in real-time decision-making and improve system reliability and cost-effectiveness in diverse applications.